

This article was downloaded by:

On: 31 January 2011

Access details: *Access Details: Free Access*

Publisher *Taylor & Francis*

Informa Ltd Registered in England and Wales Registered Number: 1072954 Registered office: Mortimer House, 37-41 Mortimer Street, London W1T 3JH, UK



## Molecular Simulation

Publication details, including instructions for authors and subscription information:

<http://www.informaworld.com/smpp/title~content=t713644482>

### Resonance frequency distribution of cantilevered (5,5)(10,10) double-walled carbon nanotube with different intertube lengths

Jeong Won Kang<sup>a</sup>; Oh Kuen Kwon<sup>b</sup>; Ho Jung Hwang<sup>c</sup>; Qing Jiang<sup>d</sup>

<sup>a</sup> Department of Computer Engineering, Chungju National University, Chungju, Republic of Korea <sup>b</sup>

Department of Electronic Engineering, Semyung University, Jecheon, Republic of Korea <sup>c</sup> School of

Electrical and Electronic Engineering, Chung-Ang University, Seoul, Republic of Korea <sup>d</sup> Department

of Mechanical Engineering, University of California, Riverside, CA, USA

Online publication date: 28 January 2011

**To cite this Article** Kang, Jeong Won , Kwon, Oh Kuen , Hwang, Ho Jung and Jiang, Qing(2011) 'Resonance frequency distribution of cantilevered (5,5)(10,10) double-walled carbon nanotube with different intertube lengths', *Molecular Simulation*, 37: 1, 18 – 22

**To link to this Article:** DOI: 10.1080/08927022.2010.509862

**URL:** <http://dx.doi.org/10.1080/08927022.2010.509862>

PLEASE SCROLL DOWN FOR ARTICLE

Full terms and conditions of use: <http://www.informaworld.com/terms-and-conditions-of-access.pdf>

This article may be used for research, teaching and private study purposes. Any substantial or systematic reproduction, re-distribution, re-selling, loan or sub-licensing, systematic supply or distribution in any form to anyone is expressly forbidden.

The publisher does not give any warranty express or implied or make any representation that the contents will be complete or accurate or up to date. The accuracy of any instructions, formulae and drug doses should be independently verified with primary sources. The publisher shall not be liable for any loss, actions, claims, proceedings, demand or costs or damages whatsoever or howsoever caused arising directly or indirectly in connection with or arising out of the use of this material.

## Resonance frequency distribution of cantilevered (5,5)(10,10) double-walled carbon nanotube with different intertube lengths

Jeong Won Kang<sup>a</sup>, Oh Kuen Kwon<sup>b</sup>, Ho Jung Hwang<sup>c\*</sup> and Qing Jiang<sup>d</sup>

<sup>a</sup>Department of Computer Engineering, Chungju National University, Chungju 380-702, Republic of Korea; <sup>b</sup>Department of Electronic Engineering, Semyung University, Jecheon 390-711, Republic of Korea; <sup>c</sup>School of Electrical and Electronic Engineering, Chung-Ang University, Seoul 156-756, Republic of Korea; <sup>d</sup>Department of Mechanical Engineering, University of California, Riverside, CA 92507, USA

(Received 15 December 2009; final version received 9 July 2010)

Analysis of ultrahigh frequency nanomechanical resonators, which are based on double-walled carbon nanotubes (DWCNTs) with various wall lengths, was carried out via classical molecular dynamics simulations. In the case of the inner wall entirely encapsulated inside the outer wall, the outer wall vibration has a significant effect on the vibration of the DWCNT; while in the case of the inner wall longer than the outer wall, the vibration of the extruded inner wall has a substantially stronger effect on the DWCNT vibration. It is shown that variations of the DWCNT resonance frequency with different wall lengths can be well fitted by Pearson VII and Gauss distribution functions. This result is potentially useful for developing design guidelines for making very fine tuners using DWCNT resonators of various wall lengths.

**Keywords:** nanotube resonator; cantilevered nanotube oscillators; molecular dynamics

### 1. Introduction

Carbon nanotubes (CNTs) exhibit appealing properties such as extremely high in-plane elastic modulus and thermal conductivity. Such properties, as well as the perfect atomic structure on the nanometer scale, imply potential applications of CNTs in nanoelectromechanical systems as components of high-frequency oscillators for sensing and signal processing applications [1–3]. A higher resonant frequency generally implies that the sensor can achieve a higher sensitivity [2]. The mechanical quality factor ( $Q$ ) also strongly influences the sensitivity of nanoelectromechanical system-based devices. For wireless communications, higher frequency resonators enable production of higher frequency filters, oscillators and mixers [4]. The advancement of high-frequency nanoelectromechanical systems is resulting in a variety of new applications including mechanical mass or charge detectors [3,5] and nanodevices for high-frequency signal processing [6] and biological imaging [7]. For example, Poncharal et al. [3] demonstrated how to exploit the resonance of a cantilevered CNT to estimate the mass of an attached carbonaceous particle as light as 30 fg, inside a transmission electron microscope. Recently, Jensen et al. [2] demonstrated a room temperature, CNT-based nanomechanical resonator with atomic mass resolution, which is based on a nanotube radio receiver design [8].

Chiu et al. [9] addressed atomic-scale mass sensors using suspended CNT resonators.

Double-walled CNT (DWCNT) resonators have different mechanical structures than single-walled carbon nanotube (SWCNT) resonators, due to their interlayer interactions, characterised by the van der Waals (vdW) potential for carbon. Jiang et al. [10] studied the energy dissipation of cantilevered SWCNT oscillators using classical molecular dynamics (MD) simulations. They confirmed that the weak interlayer binding strength contributes significantly to the energy dissipation in DWCNT. Recent technological advances have enabled DWCNTs with different wall lengths to be synthesised by various techniques. A DWCNT with a short outer wall can be fabricated via thinning and opening of the DWCNT by oxidation using carbon dioxide [11], and burning of the outer wall using an electric current [12]. A DWCNT with a short inner wall can be fabricated via the nano-peapod-to-DWCNT transition [13–16]. Bandow et al. [13,14] and Luzzi and Smith [15] have prepared DWCNTs by merging chains of C<sub>60</sub> molecules inside SWCNTs. Due to polymerisation of C<sub>60</sub> short CNTs with diameters of  $\approx 7$  Å are preferentially formed first; via heating or electron irradiation, these short CNTs subsequently merge and lengthen. During merging, a diameter transformation of the inner tube is needed in order to adjust the interlayer spacing between the inner and outer CNTs to fit the vdW

\*Corresponding author. Email: hjhwang@cau.ac.kr

distance. As a result, the number of diameter  $\approx 7 \text{ \AA}$  tubes decreases, and the number of larger diameter CNTs increases with increasing heating time [14].

Therefore, cantilevered DWCNT resonators with different wall lengths can be considered as alternative high-frequency resonators. Our previous works [17,18], based on a few cases with severe limitations, have suggested that the fundamental frequencies of DWCNT resonators can be estimated by a Gaussian distribution. The present effort is aimed at studying the frequency dependence of DWCNT resonators upon the wall lengths in a general setting. We have thus performed a systematic analysis of the resonance frequencies of cantilevered (5,5)(10,10) DWCNT resonators having a commensurate interlayer lattice matching with an interwall spacing of  $3.4 \text{ \AA}$  and different wall lengths via classical MD simulations. Our analysis shows a novel property of the fundamental frequency variations with the wall lengths.

## 2. Schematics and simulation methods

Figure 1 shows the simple schematics of a dual-telescoping cantilevered CNT resonator. By controlling the bias of the gate electrode, the telescoped cantilevered CNT can be vibrated as studied in the previous work [2,3], and then the vibrating CNT tip can be detected by the anode electrode [2]. When we want to change the vibrating frequency of the CNT tip, the desired frequency can be achieved by changing the length of the vibrating CNT by manipulating two nano-positioning controllers. We presented the schematics of a gigahertz tuner, which can be used repeatedly, based on a telescoped multi-walled CNT by manipulating a nano-positioning controller in our previous work [19]. Specially, cantilevered DWCNT resonators with different wall lengths had a wide range of the operating frequencies [17,18].

The CNT structure of our resonator is very similar to that of previous CNT-based oscillators described by Legoas et al. [20]; in both systems, the operating frequencies can be determined by both the length of the CNTs and the different wall lengths [17,18,20,21]. However, the mechanisms of the frequency generation

are different: our resonator is operated by the vibrating cantilevered CNT, whereas the previous CNT oscillators are operated by the translational oscillations based on the interwall sliding with an ideal low friction.

In order to investigate cantilevered (5,5)(10,10) DWCNT resonators, we used classical MD methods to model the oscillation behaviour of the DWCNT. Interactions between carbon atoms that form covalent bonds on CNT were modelled using the Tersoff–Brenner potential [22,23], which has been extensively applied to carbon systems [24] and is responsible for the experimental effectiveness of the simulation results [25]. The long-range interactions of carbon were characterised using the Lennard-Jones 12-6 (LJ12-6) potential, based on the parameters obtained by Ulbricht et al. [26]. In this work, the respective parameters of the LJ12-6 potential were  $\epsilon_{\text{carbon}} = 2.4038 \times 10^{-3} \text{ eV}$  and  $\sigma_{\text{carbon}} = 3.37 \text{ \AA}$ , and the cut-off distance of the LJ12-6 potential was  $10 \text{ \AA}$ . The MD methods utilised in our previous works [27–30] were implemented using the velocity Verlet algorithm, a Gunsteren–Berendsen thermostat to control the temperature and neighbour lists to improve the computing performance. The MD time step was  $5 \times 10^{-4} \text{ ps}$ . The initial atomic velocities were determined according to the Maxwell distribution, and the magnitudes were adjusted in order to fit the temperature of the system. In all the MD simulations, the temperature was set to 1 K.

The lengths of the inner (5,5) and outer (10,10) walls are denoted by  $L_5$  and  $L_{10}$ , respectively. The left ends of both walls were fixed during the classical MD simulations. The length ( $L_5$ ) of the inner (5,5) CNT was changed in 1 nm steps from 0 to 10 nm, and the lengths ( $L_{10}$ ) of the outer (10,10) CNT were also changed in 1 nm steps from 0 to 10 nm. So, we performed MD simulations of 120 cases. In order to obtain the resonant frequencies, we performed MD simulations under an external force of  $0.001 \text{ eV/\AA}$  per atom applied along the transverse direction for an initial time of 2.5 ps. Upon removal of the bending force, the CNT resonators were allowed to oscillate freely. The fundamental resonance frequencies ( $f$ ) were analysed via the fast Fourier transform, based on the data sampled at 0.05 ps [18].

## 3. Results and discussion

Figure 2(a) and (b) shows the resonance frequencies as functions of  $L_5$  and  $L_{10}$  and the contour of the resonance frequencies for  $L_5$  and  $L_{10}$ , respectively. The peak occurs at the DWCNT with the length of 1 nm, and the resonance frequencies are greatly decreased with increasing length of  $L_5$  and/or  $L_{10}$ . The ridge on the resonance frequency plot occurs from the peak to point when  $L_{10} = 7 \text{ nm}$ .

For a detailed comparison, the resonance frequencies are plotted as a function of  $L_5$  and  $L_{10}$ , as shown in Figures

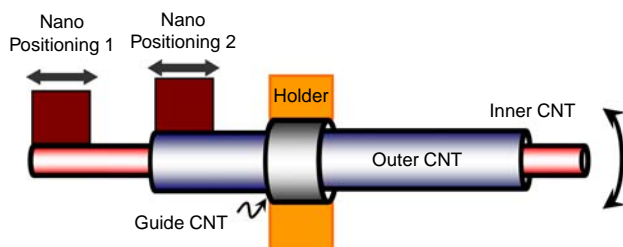


Figure 1. Simple schematics of a dual-telescoping cantilevered CNT resonator.

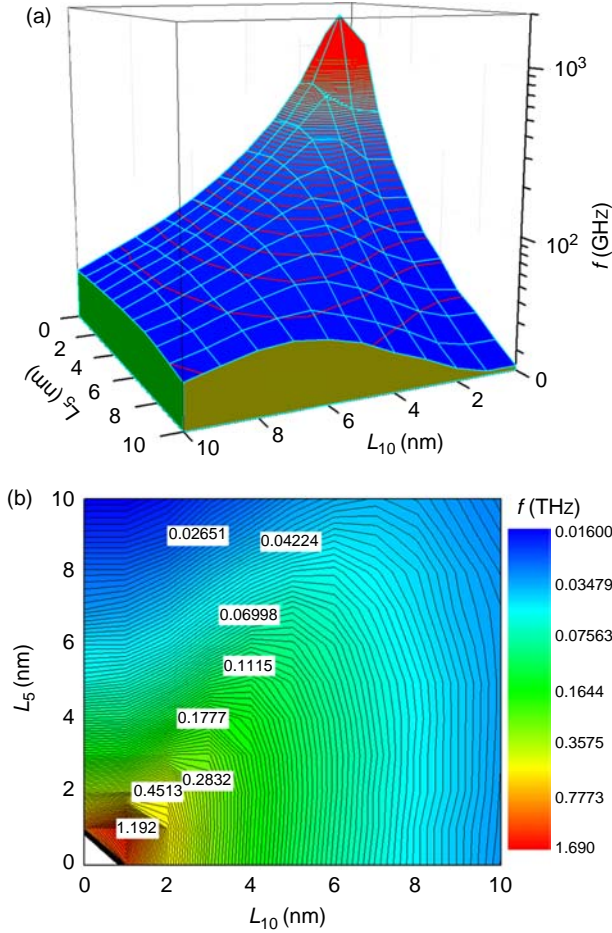


Figure 2. (a) Resonance frequencies as functions of  $L_5$  and  $L_{10}$ . (b) Contour of the resonance frequencies for  $L_5$  and  $L_{10}$ .

3 and 4, respectively. As seen in the figures, oscillators made of (5,5) and (10,10) SWCNTs or (5,5)(10,10) DWCNTs have their frequencies increase with the increasing wall length – a trend consistent with the classical beam vibration theory. However, the frequency variation with one length, while fixing the other, cannot be modelled by a regressive equation, contrary to the classical theory.

In Figure 3, the resonance frequencies are almost constant when  $L_5 \leq L_{10}$ , whereas decreasing resonance frequencies follow the frequency decrease trend of SWCNTs with increasing  $L_5$  when  $L_5 > L_{10}$ . These results show that when the inner wall is entirely encapsulated inside the outer wall, the vibration of the DWCNT is greatly influenced by the vibration of the outer wall. However, we note that the encapsulated inner wall is slightly influenced by the vibration of the corresponding DWCNT with the vdW interaction. So, the resonance frequency of the DWCNT is reduced by 15% rather than the resonance frequency of the SWCNT for the outer wall, as discussed in a previous work [18].

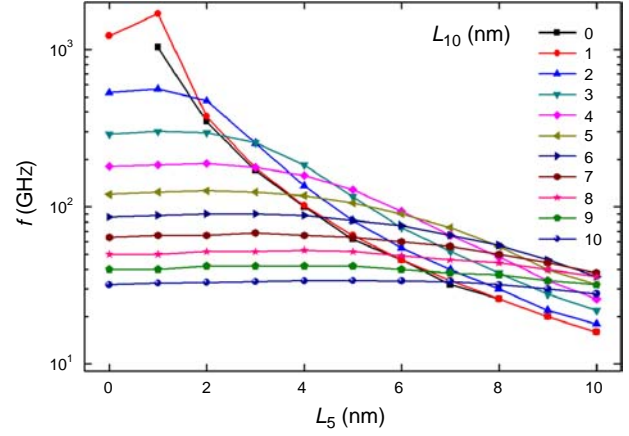


Figure 3. Resonance frequencies as a function of  $L_5$  for various values of  $L_{10}$ .

In Figure 4, for most cases, the resonance frequencies increased when  $L_{10} \leq 0.7L_5$  whereas decreasing resonance frequencies follow the frequency decrease trend of SWCNTs with increasing  $L_{10}$  when  $L_{10} > 0.7L_5$ . These results show that when the inner wall is partially covered by the outer wall, the vibration of the uncovered inner wall greatly influences the vibrational frequency of the DWCNT.

In our MD simulations, the left ends of both the inner and outer walls were fixed, whereas the other ends were free. The right free end of the outer wall can be considered as another boundary of the inner wall. The short outer wall is more rigid than the long inner wall; so, the outer wall end moves much less than the inner wall end. Thus, the semi-free boundary condition due to the free end of the outer wall is very important for understanding the vibrations of the cantilevered DWCNT resonator. This property is very important for understanding the resonance frequency variation of DWCNT resonators as a function of the outer wall length. For DWCNT resonators with short

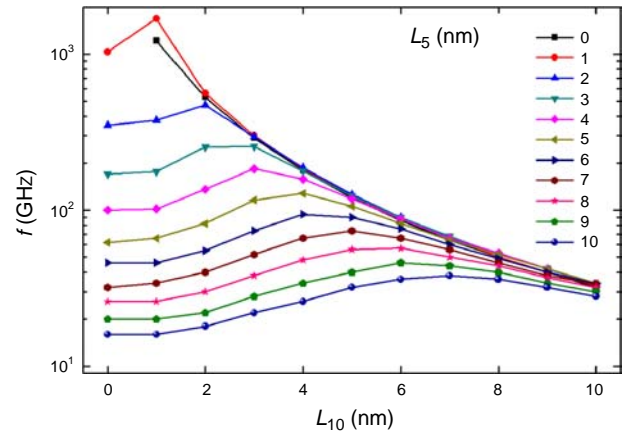


Figure 4. Resonance frequencies as a function of  $L_{10}$  for various values of  $L_5$ .



outer walls, as the length of the outer wall that covers the inner wall increases, the distance from the free end of the outer wall to that of the inner wall decreases, and this results in an increase of the fundamental resonance frequency. However, as the length of the outer wall increasingly lengthens, that of the uncovered inner wall shortens. In this case, the semi-free boundary has an increasingly smaller impact. This is understood in terms of the decrease of the fundamental resonant frequency after the peak, as shown in Figure 4. Therefore, the resonance frequencies of DWCNT resonators with short outer walls can be understood in terms of both those of the DWCNT resonator and the SWCNT resonator with the length of  $L'_5$  ( $L_5 - L_{10}$ ) under the condition of a non-fixed but limited left end. The movable right end of the outer wall can be considered as a non-fixed but limited node for the vibration of the inner wall with the length of  $L'_5$ .

From the data in Figures 3 and 4, the above discussion implies that the resonance frequencies of DWCNTs can be modelled in terms of the relationships between  $L_5$  and  $L_{10}$ . Therefore, we plot the values ( $f/f_{\text{MAX}}$ ) – the resonant frequency of a DWCNT oscillator normalised by its maximum frequency ( $f_{\text{MAX}}$ ), in Figure 5, as a function of the length ratio  $L_5/L_{10}$  for different values of the outer wall length  $L_{10}$ . The peak is at  $L_5/L_{10} = 0.76 \pm 0.04$ , and as shown by the solid line in Figure 5, the data are best fitted by the Pearson VII function, which is summarised by the centre peak point ( $x_c$ ) of 0.76099, amplitude ( $A$ ) of 955.4731, width ( $w$ ) of 1.2562 and factor ( $m$ ) of 0.50067. However, when  $0.2 \leq L_5/L_{10} \leq 1.3$  the data are well fitted by the normal distribution function, and the data when  $0.76 \leq L_5/L_{10}$  are well fitted by an exponential function. Figure 6 shows  $f/f_{\text{MAX}}$  as a function of  $L_{10}/L_5$  for different values of  $L_5$ . As shown by the solid line in Figure 6, the data are best fitted by a Gauss distribution function, which is summarised by the mean ( $x_c$ ) of 0.43147, amplitude ( $A$ ) of 2.13025, standard deviation ( $\sigma$ ) of 1.7771 and offset of

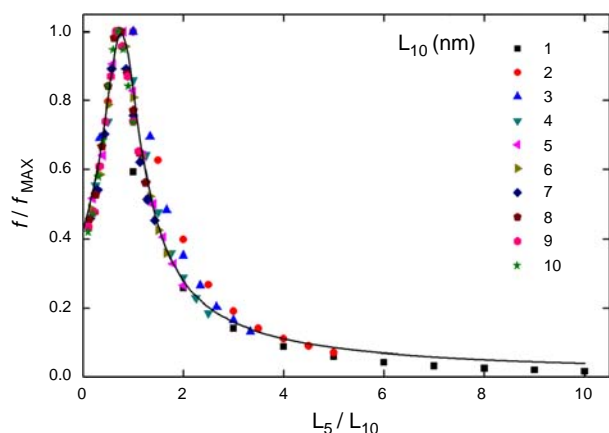


Figure 5.  $f/f_{\text{MAX}}$  as a function of  $L_5/L_{10}$  for various values of  $L_{10}$ . The solid line is a Pearson VII function.

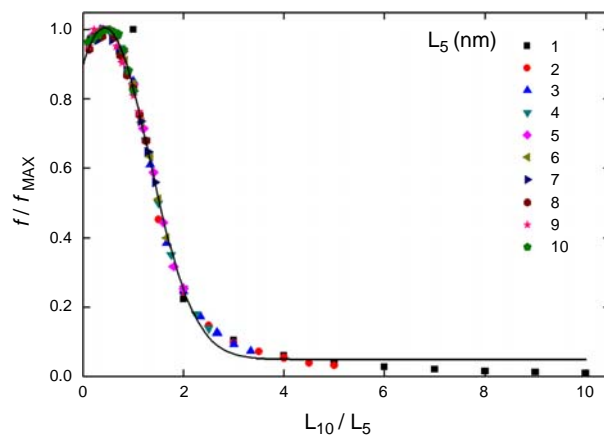


Figure 6.  $f/f_{\text{MAX}}$  as a function of  $L_{10}/L_5$  for values various of  $L_5$ . The solid line is a Gauss distribution function.

0.04943. However, the data when  $0.9 \leq L_5/L_{10}$  are well fitted by an exponential function.

These results lead us to suggest that the vibration frequencies of DWCNT resonators with different inter-wall lengths can be modelled by universal functions that are estimated by the ratio between the two lengths; so it is possible that these properties can enable us to utilise DWCNT resonators. Such a Pearson VII or a Gaussian distribution implies that the frequency of DWCNT resonators with different walls lengths is a maximum when the length of the outer wall is about 76% that of the inner wall. This property implies that DWCNT resonators with short outer walls have a high potential for engineering applications. If the length of the outer wall can be controlled independently of the inner wall, various frequency devices can be fabricated from a single type of DWCNT with walls of equal length [18].

In our MD results, the resonance frequencies of DWCNTs with walls of equal length are higher than those of DWCNTs composed of its inner walls, and slightly less than those of SWCNTs composed of its outer walls. These results are in good agreement with previous works [18,31] in which SWCNTs have larger vibration frequencies than DWCNTs. This is because the vibrational properties in the case of DWCNTs are largely affected by the inter-wall interactions due to the vibration deflections of the inner and outer nanotubes. When the outer and inner wall lengths are equal, the vibration frequencies of the former are higher than those of the latter. Therefore, slowly deflective inner walls can affect the deflective vibration of the outer wall and so such non-coaxial intertube vibration phenomena ensure that the vibration frequencies of DWCNTs are less than those of SWCNTs with a given length and diameter. The interaction between the inner and outer nanotubes of DWCNTs is considered to be coupled via the vdW force.

This work implies the potential of an alternative application of DWCNTs, as ultrahigh frequency nanome-

chanical resonators controlled by the outer or inner wall length. Such ultrahigh frequency nanomechanical resonators will facilitate the development of fast scanning probe microscopes, magnetic resonant force microscopes, and even mechanical supercomputers, ultrahigh frequency tuners, and nanodevices for high-frequency signal processing and biological imaging. When the length of the outer wall can be controlled, various resonators with different frequencies can be fabricated from several DWCNTs with walls of equal length.

#### 4. Concluding remarks

We have investigated ultrahigh frequency nanomechanical resonators, made of DWCNTs with various wall lengths, via classical MD simulations, and we have aimed our analysis on the frequency variations of these resonators with the DWCNT wall lengths. The results show that the variations can be well fitted by either the Pearson VII function when the resonant frequency of normalised by its maximum frequency is plotted as a function of the inner/outer wall length ratio  $L_5/L_{10}$  for different values of the outer wall length  $L_{10}$ , or a Gauss distribution function when the resonant frequency of normalised by its maximum frequency is plotted as a function of the outer/inner wall length ratio for different values of the inner wall length. We anticipate that these phenomena will be empirically confirmed.

#### Acknowledgements

This research was supported by the Basic Science Research Programme through the National Research Foundation of Korea (NRF) funded by the Ministry of Education, Science and Technology (2010-0015454).

#### References

- [1] C. Li and T.-W. Chou, *Single-walled carbon nanotubes as ultrahigh frequency nanomechanical resonators*, Phys. Rev. B 68 (2003), 073405.
- [2] K. Jensen, K. Kim, and A. Zettl, *An atomic-resolution nanomechanical mass sensor*, Nat. Nanotechnol. 3 (2008), pp. 533–537.
- [3] P. Poncharal, Z.L. Wang, D. Ugarte, and W.A. de Heer, *A carbon nanotube field-emission electron source*, Science 283 (1999), pp. 1513–1516.
- [4] H.J. De Los Santos, *Introduction to Microelectromechanical Microwave Systems*, Artech House Publishers, London, 1999.
- [5] A.N. Cleland and M.L. Roukes, *A nanometre-scale mechanical electrometer*, Nature 392 (1998), pp. 160–162.
- [6] A. Erbe and R.H. Blick, *Silicon-on-insulator based nanoresonators for mechanical mixing at radio frequencies*, IEEE Trans. Ultrason. Ferroelectr. Freq. Control 49 (2002), pp. 1114–1117.
- [7] T.A. Barrett, C.R. Miers, H.A. Sommer, K. Mochizuki, and J.T. Markert, *Design and construction of a sensitive nuclear magnetic resonance force microscope*, J. Appl. Phys. 83 (1998), pp. 6235–6237.
- [8] K. Jensen, J. Weldon, H. Garcia, and A. Zettl, *Nanotube radio*, Nano Lett. 7 (2007), pp. 3508–3511.
- [9] H.-Y. Chiu, P. Hung, H.W. Ch Postma, and M. Bockrath, *Atomic-scale mass sensing using carbon nanotube resonators*, Nano Lett. 8 (2008), pp. 4342–4346.
- [10] H. Jiang, M.-F. Yu, B. Liou, and Y. Huang, *Intrinsic energy loss mechanisms in a cantilevered carbon nanotube beam oscillator*, Phys. Rev. Lett. 93 (2004), 185501.
- [11] S.C. Tsang, P.J.F. Harris, and M.L.H. Green, *Thinning and opening of carbon nanotubes by oxidation using carbon dioxide*, Nature 362 (1993), pp. 520–522.
- [12] P.G. Collins, M. Hersam, M. Arnold, R. Martel, and P. Avouris, *Current saturation and electrical breakdown in multiwalled carbon nanotubes*, Phys. Rev. Lett. 86 (2001), pp. 3128–3131.
- [13] S. Bandow, M. Takizawa, K. Hirahara, M. Yudasaka, and S. Iijima, *Raman scattering study of double-wall carbon nanotubes derived from the chains of fullerenes in single-wall carbon nanotubes*, Chem. Phys. Lett. 337 (2001), pp. 48–54.
- [14] S. Bandow, T. Hiraoka, T. Yumura, K. Hirahara, H. Shinohara, and S. Iijima, *Raman scattering study on fullerene derived intermediates formed within single-wall carbon nanotube: From peapod to double-wall carbon nanotube*, Chem. Phys. Lett. 384 (2004), pp. 320–325.
- [15] D.E. Luzzi and B.W. Smith, *Carbon cage structures in single wall carbon nanotubes: A new class of materials*, Carbon 38 (2000), pp. 1751–1753.
- [16] W. Mickelson, S. Aloni, W.-Q. Han, J. Cumings, and A. Zettl, *Packing  $C_{60}$  in boron nitride nanotubes*, Science 300 (2003), pp. 467–469.
- [17] J.W. Kang, O.K. Kwon, J.H. Lee, Y.G. Choi, and H.J. Hwang, *Frequency change by inter-walled length difference of double-wall carbon nanotube resonator*, Solid State Comm. 149 (2009), pp. 1574–1577.
- [18] J.W. Kang, Y.G. Choi, Y. Kim, Q. Jiang, O.K. Kwon, and H.J. Hwang, *Frequency of cantilevered double-wall carbon nanotube resonator as a function of outer wall length*, J. Phys.: Condens. Matter 21 (2009), 385301.
- [19] J.W. Kang, K.R. Byun, O.K. Kwon, Y.G. Choi, and H.J. Hwang, *Gigahertz frequency tuner of telescoping double-walled carbon nanotube: Molecular dynamics simulations*, Mol. Simul. 36 (2010), pp. 418–424.
- [20] S.B. Legoas, V.R. Coluci, S.F. Braga, P.Z. Coura, S.O. Dantas, and D.S. Galvão, *Molecular-dynamics simulations of carbon nanotubes as gigahertz oscillators*, Phys. Rev. Lett. 90 (2003), 055504.
- [21] J.W. Kang and H.J. Hwang, *Nanotube oscillators: Properties and applications*, J. Comput. Theor. Nanosci. 6 (2009), pp. 2347–2379.
- [22] J. Tersoff, *Modeling solid-state chemistry: Interatomic potentials for multicomponent systems*, Phys. Rev. B 39 (1989), pp. 5566–5568.
- [23] D.W. Brenner, *Empirical potential for hydrocarbons for use in simulating the chemical vapor deposition of diamond films*, Phys. Rev. B 42 (1990), pp. 9458–9471.
- [24] C. Li, E.T. Thostenson, and T.-W. Chou, *Sensors and actuators based on carbon nanotubes and their composites: A review*, Composites Sci. Tech. 68 (2008), pp. 1227–1249.
- [25] S.B. Sinnott and R. Andrews, *Carbon nanotubes: Synthesis, properties, and applications*, Crit. Rev. Solid State Mater. Sci. 26 (2001), pp. 145–249.
- [26] H. Ulbricht, G. Moos, and T. Hertel, *Interaction of  $C_{60}$  with carbon nanotubes and graphite*, Phys. Rev. Lett. 90 (2003), 095501.
- [27] J.W. Kang, C.S. Won, G.H. Ryu, Y.G. Choi, and H.J. Hwang, *Molecular dynamics simulations of inertia sensor with carbon nanotube oscillators*, J. Nanosci. Nanotechnol. 9 (2009), pp. 6943–6947.
- [28] J.W. Kang, Y.G. Choi, and J.H. Lee, *Molecular dynamics simulations of an angular velocimeter with a carbon nanotube oscillator*, J. Korean Phys. Soc. 55 (2009), pp. 46–49.
- [29] J.W. Kang, D.Y. Kang, Y.G. Choi, S. Lee, and H.J. Hwang, *Molecular dynamics study of tunable double-walled carbon nanotube oscillator*, J. Comput. Theor. Nanosci. 6 (2009), pp. 1580–1584.
- [30] J.W. Kang, J.H. Lee, K.-S. Kim, and Y.G. Choi, *Molecular dynamics simulation study on capacitive nano-accelerometers based on telescoping carbon nanotubes*, Model. Simul. Mater. Sci. Eng. 17 (2009), 025011.
- [31] T. Natsuki, Q.-Q. Ni, and M. Endo, *Analysis of the vibration characteristics of double-walled carbon nanotubes*, Carbon 46 (2008), pp. 1570–1573.